Cancer Research

AACR

Cell-Permeable NM23 Blocks the Maintenance and Progression of Established Pulmonary Metastasis

Junghee Lim, Giyong Jang, Seeun Kang, et al.

Updated Version	Access the most recent version of this article at: doi:10.1158/0008-5472.CAN-11-2015
Supplementary Material	Access the most recent supplemental material at: http://cancerres.aacrjournals.org/content/suppl/2011/11/30/0008-5472.CAN-11-2015.DC1.html

Cited Articles	This article cites 40 articles, 10 of which you can access for free at: http://cancerres.aacrjournals.org/content/71/23/7216.full.html#ref-list-1
Citing Articles	This article has been cited by 1 HighWire-hosted articles. Access the articles at: http://cancerres.aacrjournals.org/content/71/23/7216.full.html#related-urls

E-mail alerts	Sign up to receive free email-alerts related to this article or journal.
Reprints and Subscriptions	To order reprints of this article or to subscribe to the journal, contact the AACR Publications Department at pubs@aacr.org.
Permissions	To request permission to re-use all or part of this article, contact the AACR Publications Department at permissions@aacr.org.

Cell-Permeable NM23 Blocks the Maintenance and Progression of Established Pulmonary Metastasis

Junghee Lim[1,3], Giyong Jang[1], Seeun Kang[1], Guewha Lee[1], Do Thi Thuy Nga[2], Do Thi Lan Phuong[2], Hyuncheol Kim[3], Wael El-Rifai[4], H. Earl Ruley[5], and Daewoong Jo[1,2,4]

Abstract

Occult metastases are a major cause of cancer mortality, even among patients undergoing curative resection. Therefore, practical strategies to target the growth and persistence of already established metastases would provide an important advance in cancer treatment. Here, we assessed the potential of protein therapy using a cell permeable NM23-H1 metastasis suppressor protein. Hydrophobic transduction domains developed from a screen of 1,500 signaling peptide sequences enhanced the uptake of the NM23 protein by cultured cells and systemic delivery to animal tissues. The cell-permeable (CP)-NM23 inhibited metastasis-associated phenotypes in tumor cell lines, blocked the establishment of lung metastases, and cleared already established pulmonary metastases, significantly prolonging the survival of tumor-bearing animals. Therefore, these results establish the potential use of cell-permeable metastasis suppressors as adjuvant therapy against disseminated cancers. *Cancer Res; 71(23); 7216–25. ©2011 AACR.*

Introduction

Metastasis is an acquired and separately evolving phenotype that enables cancer cells to disseminate and grow at locations distant from the primary tumor site. For many tumors, the molecular changes responsible for initiating metastatic spread have already occurred by the time of initial diagnosis, and are ultimately responsible for most cancer deaths (1, 2). Effective strategies to target disseminated tumors are therefore expected to have tremendous therapeutic benefit.

In principle, antimetastasis therapies could either block activities required for the growth or survival of disseminated cancer cells or restore the expression and/or activity of proteins that function to suppress metastasis. The latter includes more than 20 metastasis suppressors—proteins that selectively inhibit the seeding, growth, or persistence of metastatic foci while having only limited effects on primary tumors (3). NME1, the first reported metastasis suppressor gene, was initially characterized as nucleoside diphosphate kinase (NDK), an enzyme required to maintain cellular pools of nucleoside triphosphates. Interest in NDK as a metastasis suppressor (alternatively named NM23-H1 or NM23) was prompted by studies describing inverse correlations between NM23 expression and metastatic potential, first in melanoma cells (4) and later in other types of tumors (5). Subsequent gene transfer experiments documented the ability of NM23 to suppress metastasis-associated phenotypes both in cultured cells and in animal metastasis models (6–10). The precise mechanism by which NM23 influences metastasis is not understood, in part, because the protein possesses multiple enzymatic activities that directly or indirectly suppress mitogen-activated protein kinase (MAPK) signaling (11, 12); regulate small G-protein functions important in cell motility, cytoskeletal reorganization, and cell adhesion (13–15); and influence genome maintenance (16, 17). Nevertheless, clinical trials based on hormonal activation of endogenous NM23 expression are currently in progress (4).

In the present study, we describe an antimetastasis therapy based on the systemic delivery of a cell penetrating NM23-H1 protein. For this experiment, we developed novel macromolecule transduction domains (MTD) modeled after hydrophobic signal peptides previously shown to promote protein uptake by cultured cells and animal tissues (18). The MTD-NM23 inhibited metastasis-associated phenotypes in tumor cell lines and not only suppressed the establishment of lung metastases but also cleared previously established metastases, significantly prolonging the survival of animals harboring disseminated tumor cells.

Authors' Affiliations: [1]ProCell R&D Institute, ProCell Therapeutics, Inc., Seoul; [2]Department of Biomedical Sciences, Chonnam National University Medical School, Gwangju; and [3]Interdisciplinary Program of Integrated Biotechnology, Sogang University, Seoul, Korea; and Departments of [4]Surgery and Cancer Biology and [5]Microbiology and Immunology, Vanderbilt University School of Medicine, Nashville, Tennessee

Corresponding Author: Daewoong Jo, Department of Surgery, Vanderbilt University School of Medicine 1255 MRB IV, 2215B Garland Avenue, Nashville, TN 37232. Phone: 615-322-8207; Fax: 615-322-7852; E-mail: dae-woong.jo@vanderbilt.edu

American Association for **Cancer Research**

Figure 1. Inhibition of MAPK signaling and EDG2 expression by CP-NM23. MDA-MB-435 (A), MDA-MB-231 (B), and A549 cells (C) were treated for 1 hour with 10 μmol/L of the indicated recombinant NM23 proteins. Cell lysates, prepared immediately (p-MEK and p-ERK) or after 8 hours (EDG2) were immunoblotted with antibodies against the indicated proteins. ERK, extracellular signal-regulated kinase; MEK, MAP/ERK kinase.
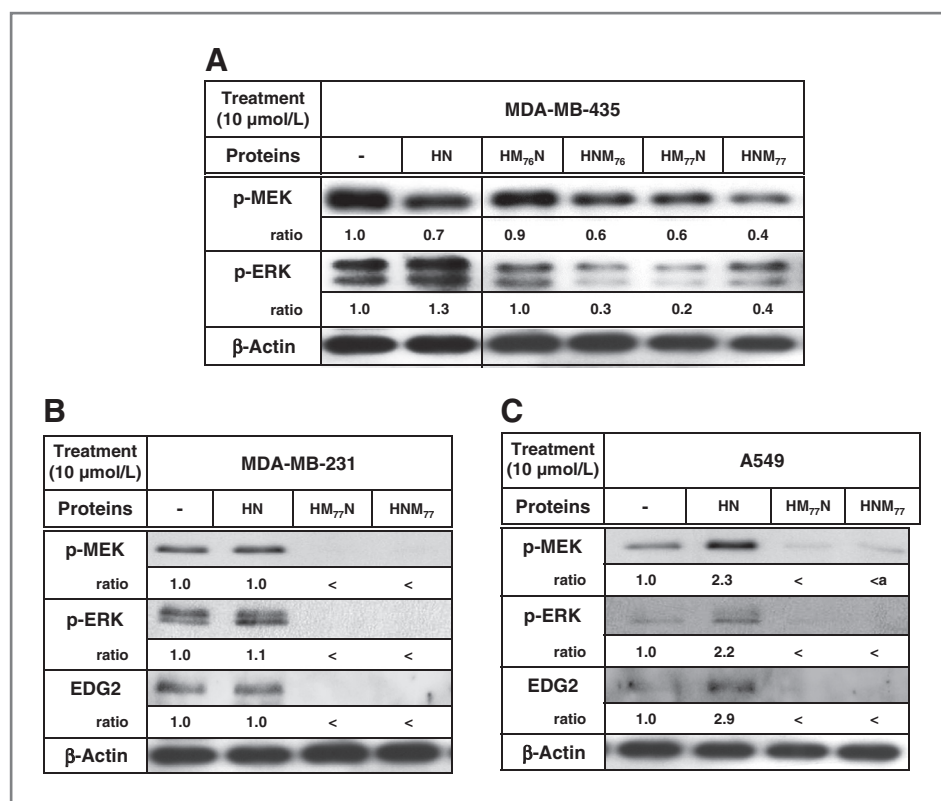
Materials and Methods

Preparation of recombinant MTD-fused proteins

MTD-76 and MTD-77 were identified from a screen of 1,500 signaling peptides for sequences with protein transduction activity. Sequences spanning amino acids 8 to 30 of NP631283 (FLIAGVIVALLAVFTVVRAVRIV) and 1 to 23 of NP003231 (MWPLWLCWALWVLPLAGPGAALT) were subsequently modified (D. Jo et al.; manuscript in preparation), generating ALVLPLAP and AVALLILAV, respectively. Coding sequences for NM23 and enhanced GFP (EGFP) fusion proteins were cloned into pET-28a$^+$ (Novagen) from PCR-amplified DNA segments (Supplementary Table S1). The recombinant proteins were purified from *Escherichia coli* BL21-CodonPlus (DE3) cells grown at an A_{600} of 0.6 and induced for 2 hours with 0.7 mmol/L Isopropyl β-D-1-thiogalactopyranoside (IPTG). Denatured ×6 histidine-tagged recombinant proteins were purified by Ni^{2+} affinity chromatography as directed by the supplier (Qiagen). After purification, they were dialyzed against a refolding buffer (0.55 mol/L guanidine HCl, 0.44 mol/L L-arginine, 50 mmol/L Tris-HCl, 150 mmol/L NaCl, 1 mmol/L EDTA, 100 mmol/L NDSB, 2 mmol/L reduced glutathione, and 0.2 mmol/L oxidized glutathione) and then against a physiologic buffer such as RPMI-1640 medium. H, N, and M stand for the His tag, NM23, and MTD, respectively. Histidine-tagged recombinant NM23 proteins were HN (His-NM23), HM$_{76}$N (His-MTD76-NM23), HNM$_{76}$ (His-MTD76-NM23), HM$_{77}$N (His-MTD77-NM23), and HNM$_{77}$ (His-NM23-MTD77).

Analysis of protein uptake in cultured cells

Recombinant proteins were conjugated to 5/6-fluorescein isothiocynate (FITC), according to the manufacturer's instructions (Pierce Chemical). RAW 264.7 cells were treated with 10 μmol/L FITC-labeled proteins for 1 hour at 37°C, washed 3 times with cold PBS, treated with proteinase K (10 μg/mL) for 20 minutes at 37°C to remove cell-surface bound proteins, and subjected to FACS analysis (FACSCalibur; Becton Dickinson). Each experiment was conducted at least 3 times.

Experiments to visualize protein uptake were conducted in much the same manner except that NIH3T3 cells were exposed to 10 μmol/L FITC-proteins for 30 minutes and then nuclei or plasma membranes were counter stained with 1 μg/mL propidium iodide (Sigma-Aldrich) or 5 μg/mL FM4-64 (Molecular Probes), respectively. The cells were washed 3 times with cold PBS and examined by confocal laser scanning microscopy.

Systemic delivery of MTD fusion proteins

Six-week-old Balb/c female mice were injected intraperitoneally (300 μg/head) with FITC only, FITC-conjugated EGFP, or NM23 recombinant proteins. After 2 hours, the liver, kidney, spleen, lung, heart, and brain were isolated, infused with O.C.T. compound (Sakura), and frozen on dry ice. Cryosections (20-μm thickness) were analyzed by fluorescence microscopy. Alternatively, the uptake of FITC-NM23 proteins was assessed after 1 and 2 hours by fluorescence-activated cell sorting (FACS) analysis of unfixed blood leukocytes/lymphocytes or total splenocytes.
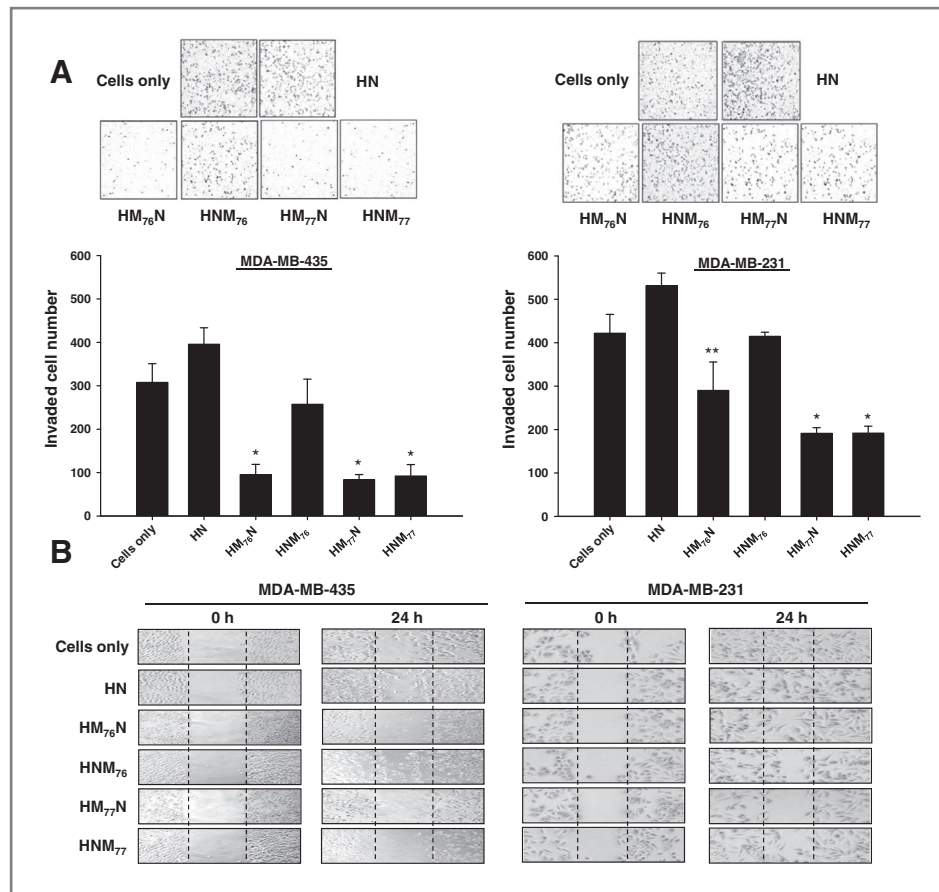
Figure 2. CP-NM23 suppresses cell invasion and migration. A, Matrigel invasion assay. Tumor cells were treated for 1 hour with the indicated proteins (10 μmol/L); after 24 hours, cells penetrating and migrating to the basal side of Matrigel-coated membranes were visualized (top) and counted (bottom). The data are presented as means ± SD ($n = 3$), *, $P < 0.01$; **, $P < 0.05$, as determined by the Student unpaired t test. B, wound-healing assay. Cell monolayers, treated with NM23 proteins as in (A), were scraped to create a "wound" devoid of cells (dashed lines) and photographed after 24 hours. Data shown here are representative of 5 independent assays.

To determine the tissue distribution of cell permeable (CP)-NM23 proteins, mice were injected i.v. with diluent, HN, or MTD-NM23 (600 μg/mouse). The spleen and liver were removed after 3 hours, embedded in paraffin, sectioned at 5 μmol/mL, and immunostained with NM23 (Santa Cruz Biotechnology) or ×6 His tag (Abcam) monoclonal antibodies, followed by HRP-conjugated goat anti-mouse secondary antibody (Santa Cruz).

Immunoblot analysis

MDA-MB-435, MDA-MB-231, and A549, HCT116 cell lines were purchased from the Korean Cell Line Bank (Seoul, Korea) and American Type Culture Collection (ATCC), respectively and maintained as recommended by the suppliers. The biologic activities of the cell lines (MDA-MB-435, MDA-MB-231, and HCT116) were authenticated by *in vivo* metastasis and/or tumor growth in Balb/c *nu/nu* mice. All cell lines were negative for mycoplasma assessed by MycoALERT (2009; Lonza). Cells were treated at 37°C with 10 μmol/L recombinant proteins (HN, HM₇₆N, HNM₇₆, HM₇₇N, or HNM₇₇) or with buffer only. After 1 hour, cells were processed for immunoblot analysis to detect the phosphorylation of MAP/ERK kinase (MEK), extracellular signal–regulated kinase (ERK), and p53 or incubated for an additional 8 hours to monitor changes in EDG2 and VEGF expression. Western blots were probed with antibodies against EDG2, VEGF, and β-actin (Santa Cruz) and phospho-ERK, phospho-MEK, and phospho-p53 (Cell Signaling). The secondary antibody was goat anti-mouse immunoglobulin–horseradish peroxidase (Santa Cruz).

Invasion assay

MDA-MB-435 human breast cancer cells were treated with HN, HM₇₆N, HNM₇₆, HM₇₇N, or HNM₇₇ proteins (10 μmol/L) or with buffer alone for 1 hour at 37°C. A total of 1×10^5 cells were added to the top of a trans-well chamber partitioned with a Matrigel-coated (40 μg per well; BD Biosciences) polycarbonate membrane filter (BD Falcon) with a pore size of 3 μm. After 24 hours at 37°C, the filters were washed with PBS and the noninvasive cells remaining on the surface of the upper part were removed with a cotton swab. The invasive cells that passed through the Matrigel and migrated to the lower part of the filter were fixed with 4% paraformaldehyde for 10 minutes, stained with 0.5% (w/v) hemacolor for 20 minutes, and counted with an optical microscope. Statistical significance was determined by the Student t test.

Wound-healing assay

Confluent monolayers of MDA-MB-435 cells were treated with HN, HM₇₆N and HNM₇₆, HM₇₇N or HNM₇₇ proteins (10 μmol/L) or with buffer alone for 1 hour at 37°C. After the cells were washed with PBS, they were wounded with a sterile yellow micropipette tip and cultured for 24 hours at
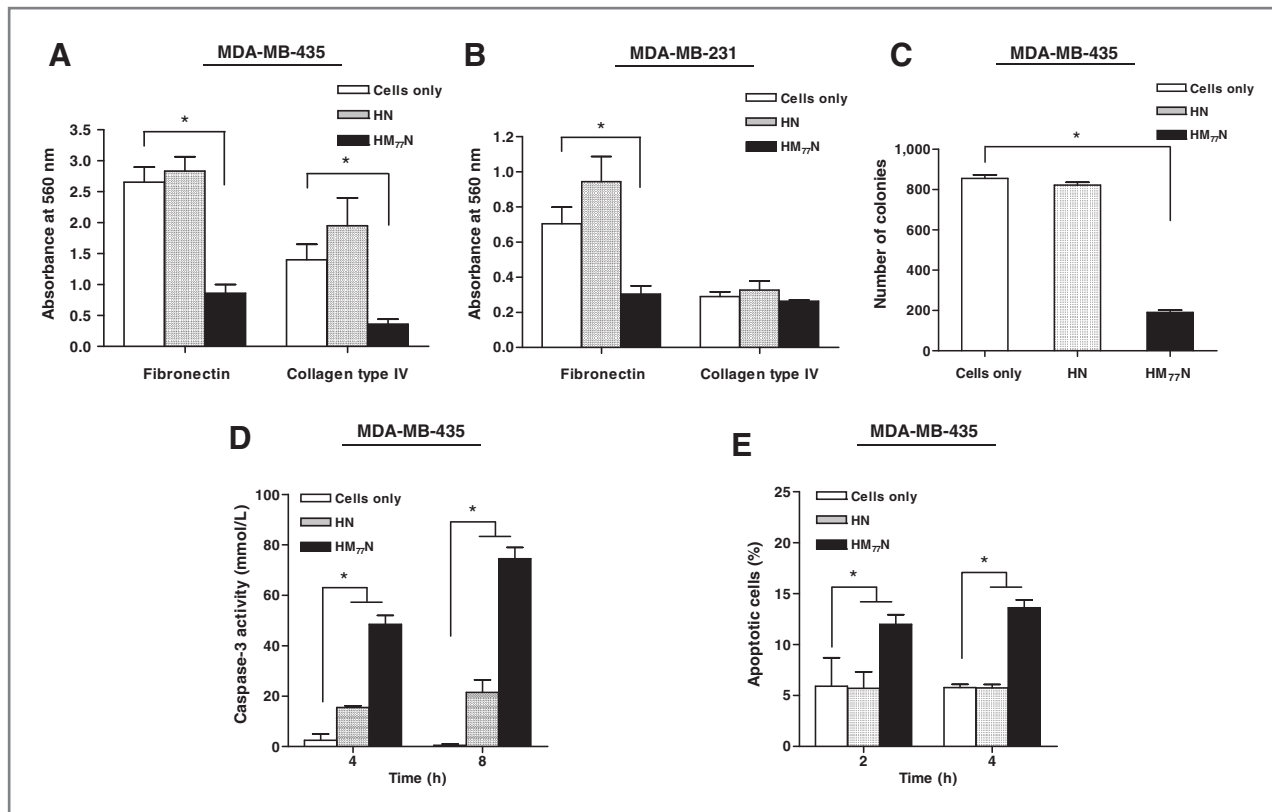
Figure 3. CP-NM23 inhibits cell adhesion and anchorage-independent growth, and induces apoptosis in cancer cells. A and B, adhesion assay. MDA-MB-435 (A) and MDA-MB-231 (B) cells were treated with 10 μmol/L of recombinant NM23 proteins (HN, gray bar; or $HM_{77}N$, black bar) or with a vehicle (cells only, white bar). Cells adhering to fibronectin or type IV collagen were assessed by absorbance at 560 nm. The data are presented as means ± SD ($n = 3$); *, $P < 0.05$; **, $P < 0.005$, Student unpaired t test. C, anchorage-independent cell growth. MDA-MB-435 cells were treated with 10 μmol/L of recombinant NM23 proteins (HN, gray bar; or $HM_{77}N$, black bar) or vehicle (cells only, white bar). Colonies larger than 3 mm in diameter were counted and presented as means ± SD ($n = 3$); *, $P < 0.005$, as determined by the Student unpaired t test. D and E, apoptosis induction by CP-NM23. CP-NM23-mediated activation of caspase-3 in cancer cells (MDA-MB-435) treated with 10 μmol/L control protein (HN, gray), CP-NM23 ($HM_{77}N$, black) or vehicle (cells only, white) for 4 or 8 hours (D). Apoptosis as assessed by Annexin V staining was determined in the cells treated with $HM_{77}N$ for 2 or 4 hours (E). The data are represented as a mean ± SD of 3 independent experiments. *, $P < 0.05$, as determined by the Student unpaired t test.

37°C. The cells were fixed in methanol for 1 minute, stained with Giemsa (Chameleon Chemical) for 5 minutes, and washed with distilled water. The migration was quantified by counting the number of cells that migrated from the wound edge into the clear area. Representative data from 3 experiments are presented.

Adhesion assay

Ninety-six–well plates were coated with 10 μg/mL fibronectin (BD Biosciences), 10 μg/mL mouse collagen IV (BD Biosciences), or 1 mg/mL BSA for 16 hours at 4°C. Wells were then washed with 1 mg/mL BSA RPMI and blocked for 1 hour with 5 mg/mL BSA RPMI at 37°C. MDA-MB-435 or MDA-MB-231 cells (2×10^4 well) were allowed to adhere for 30 minutes after treatment with 10 μmol/L of recombinant proteins (HN or $HM_{77}N$) for 24 hours. The wells were washed carefully, and adherent cells were fixed, stained with crystal violet, and dried overnight. Cells were lysed in 2% SDS solution. Cell number was estimated with a SpectraMax microplate reader (Molecular Devices) at 550 nm. Background absorbance from a

BSA-coated well was subtracted. Statistical significance was determined by the Student t test.

Anchorage-independent growth assay

A bottom agar (Difco) of 0.5% in Dulbecco's Modified Eagle's Media (DMEM) + 10% FBS was allowed to harden in all wells of a 24-well plate. Cells (MDA-MB-435) that were treated for 24 hours with 10 μmol/L of recombinant proteins (HN or $HM_{77}N$) were suspended in a 0.3% agar/RPMI + 10% FBS medium at a concentration of 1×10^4/mL. A total of 0.5 mL of each cell suspension was plated on top of the bottom agar in triplicate wells. Colony number was assessed after 14 days of growth at 37°C. Colonies larger than 3 mm in diameter were counted. This assay was done in triplicate. Statistical significance was determined by the Student t test.

Tube formation assay

Endothelial cell tube-forming assays were done in 24-well Matrigel (BD Bioscience) coated plates. Human umbilical vein
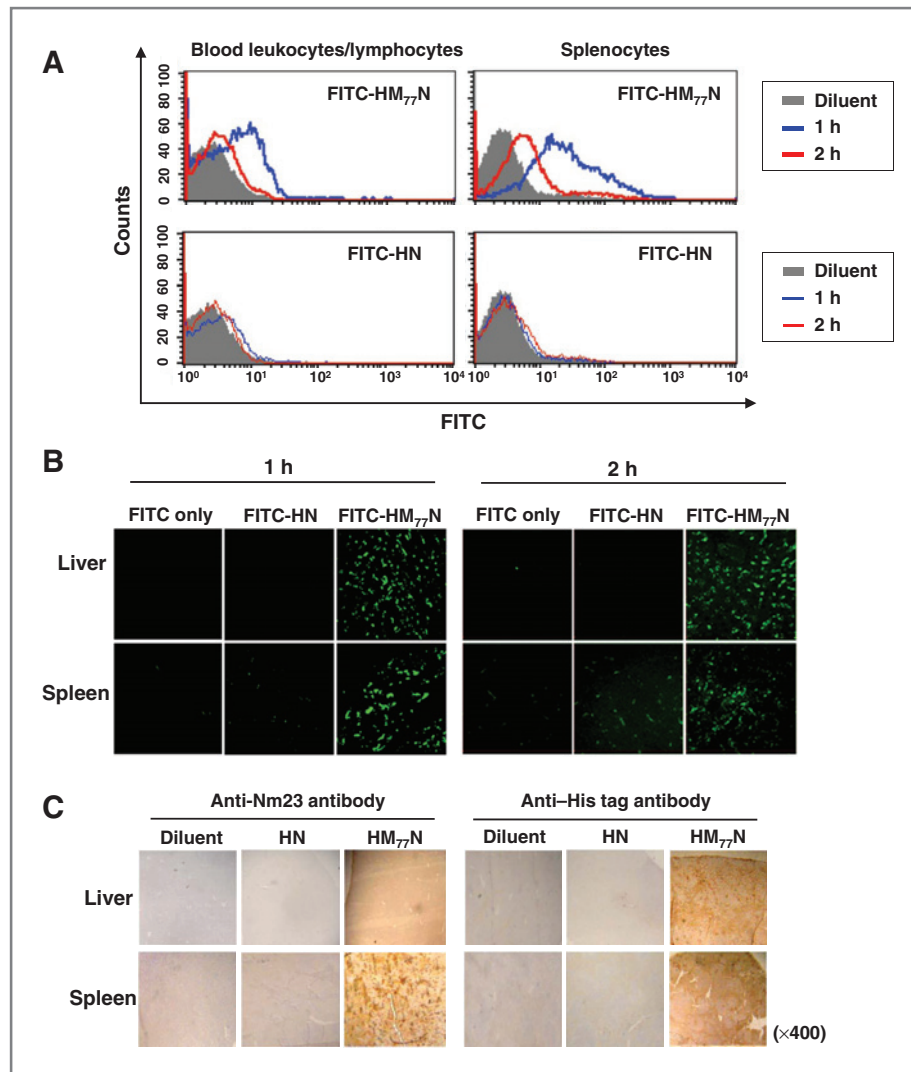
Figure 4. Systemic delivery of CP-NM23. A, mice were injected i.v. with FITC-conjugated HM$_{77}$N, HN or with dilutant alone (solid gray), and protein uptake by peripheral blood leukocytes/lymphocytes (left) or splenocytes (right) was assessed by flow cytometry after 1 (blue line) or 2 (red line) hours. B and C, tissue distribution of HM$_{77}$N at the indicated times after injection was assessed by fluorescence microscopy (B) and after 3 hours by immunostaining (C).

endothelial cells (HUVEC; 5×10^4) were treated with 5 μmol/L of recombinant protein (HN or HM$_{77}$N) for 1 hour or 12 hours and tube formation was monitored after 24 hours.

Xenograft metastasis models

Female Balb/c *nu/nu* mice were i.v. inoculated (5×10^6) with human breast cancer cells (MDA-MB-435) through the lateral tail vein. After 5 weeks, tumor metastasis-induced mice were intravenously administered with protein (300 μg/mouse) for a period of 3 weeks. There were an additional 2 weeks of observation by our group (ProCell R&D Institute) or a professional contracted research organization (Biotoxtech, Korea), and maintenance for 24 or 40 weeks for the determination of the survival rate of the mice following the termination of treatment. After protein treatment, half of the mice were killed, and 6 organs (brain, heart, lung, liver, kidney, and spleen) from each were collected and kept in a suitable fixation solution until the next step. Lung tissues were kept in Bouin's fixative solution overnight to detect metastasis. Five-micrometer formalin-fixed, paraffin-embed-

ded lung sections were immunostained with mouse anti-vimentin antibody (Abcam) followed by goat anti-mouse IgG-HRP (Santa Cruz Biotechnology).

Statistical analysis

All experimental data obtained from cultured cells are expressed as the means ± SD from at least 3 independent experiments. For the invasion assays, Annexin V assays, caspase-3 assays, anchorage-independent growth assays, and adhesion assays, statistical significance was evaluated using the one-tailed Student t test. For animal tests, paired t tests were used for comparisons between and within groups to determine the significance of the differences in survival *in vivo*. Statistical significance was established as $P < 0.05$.

Results

Protein sequences with enhanced MTD activity

Previous studies using hydrophobic MTD to deliver protein cargoes into cultured cells and animals almost exclusively used

an MTD derived from the signal peptide of fibroblast growth factor 4 (FGF-4; ref. 19–21). To identify sequences with enhanced MTD activity, we screened a library of predicted hydrophobic signal peptides for their ability to promote the uptake of FITC-labeled EGFP fusion proteins into cultured cells (D. Jo et al., manuscript in preparation). High-scoring peptides were further modified and included 2 [MTD-76 (ALVLPLAP: M_{76}) and MTD-77 (AVALLILAV: M_{77})] with greater (~2.2- and 4.0-fold respectively; Supplementary Fig. S1A and B) protein transduction activity than FGF-4 MTD (AAVLLPVL-LAAP: M_m). Conversely, a random hydrophobic peptide (SAN-VEPLERL: S) did not increase EGFP uptake. Moreover, MTD-76 and MTD-77 enhanced the systemic delivery of EGFP fusion proteins to multiple tissues following intraperitoneal injection (Supplementary Fig. S1C), suggesting that both MTDs were effective *in vitro* and *in vivo*.

CP-NM23 proteins

NM23 proteins containing MTD-76 or MTD-77 fused to either the N- or C-terminus along with an amino-terminal $6\times$ His tag were expressed in *E. coli* and purified by Ni^{2+} affinity chromatography (Supplementary Fig. S2A), with yields of soluble protein ranging from 4 to 15 mg/L. Higher levels of all MTD-NM23 fusion proteins ($HM_{76}N$, HNM_{76}, $HM_{77}N$, and HNM_{77}) accumulated in RAW cells, as compared with a control protein (His tagged NM23, HN) without an MTD sequence (Supplementary Fig. S2B); however, MTD-77 had greater transduction activity, regardless of whether the MTD was positioned on the amino or carboxyl terminal end. Given this difference, subsequent experiments focused primarily on MTD-77, which also enhanced the uptake of NM23 by RAW cells (Supplementary Fig. S2C) and systemic delivery of NM23 to various organs in mice (Supplementary Fig. S3).

CP-NM23 suppresses MAPK signaling and cell migration

The metastasis suppressor NM23 has pleiotropic effects on MAPK signaling, EDG2 (lysophosphatidic acid receptor) expression, and cell migration. We, therefore, examined the effects of CP-NM23 on steady-state MEK and ERK phosphorylation and EDG2 expression in several human tumor cell lines. Both MTD-76- and MTD-77-NM23 proteins suppressed MEK and ERK phosphorylation in MDA-MB-435 breast cancer cells (Fig. 1A), although MTD-77-NM23 proteins ($HM_{77}N$ and HNM_{77}) were more potent suppressors, consistent with higher levels of protein uptake (Supplementary Fig. S2B). The effects of $HM_{77}N$ were even more striking, with near complete suppression of MEK and ERK phosphorylation and EDG2 expression in MDA-MB-231 and A549 cells (Fig. 1B and C). These results suggest that MTD-76 and MTD-77 can deliver biologically active NM23 protein into human tumor cells.

We next used a Matrigel invasion assay to assess the effects of CP-NM23 proteins on cell migration. Tumor cells with high mobility [MDA-MB-435 (Fig. 2A, left) and MDA-MB-231 (Fig. 2A, right)] were treated with recombinant proteins for 1 hour, and their migration was compared with that of controls treated with media alone or with NM23 lacking an MTD. $HM_{76}N$, $HM_{77}N$, and HNM_{77} significantly inhibited migration in both cell lines (by 68% and 56%; 79% and 58%; and 74% and 58%,

respectively). Similar results were obtained in a wound-healing assay using the same cell lines (Fig. 2B). $HM_{77}N$, which displayed the greatest uptake and activity suppressing MAPK signaling and cell migration, was selected as the best candidate to test for antimetastasis activity.

CP-NM23 suppresses metastasis-associated phenotypes

The metastatic phenotype relies on the ability of tumor cells to adhere to distal sites, survive, and promote angiogenesis. We therefore evaluated the impact of $HM_{77}N$ on these aspects of the metastatic phenotype. First, we examined the adhesion of cancer cell lines to fibronectin and type 4 collagen, 2 major components of the extracellular matrix. $HM_{77}N$ significantly inhibited the attachment of MDA-MB-435 (Fig. 3A) and MDA-MB-231 (Fig. 3B) cells to fibronectin, and suppressed the attachment of MDA-MB-435 cells to type IV collagen. MDA-MB-231 cells adhered poorly to type 4 collagen, and attachment was not reduced further by $HM_{77}N$. $HM_{77}N$ also inhibited anchorage independent growth of MDA-MB-435 cells (Fig. 3C) and induced significant apoptosis as assessed by caspase-3 activity and Annexin V staining (Fig. 3D and E). However, $HM_{77}N$ was not overtly toxic to untransformed (NIH3T3)
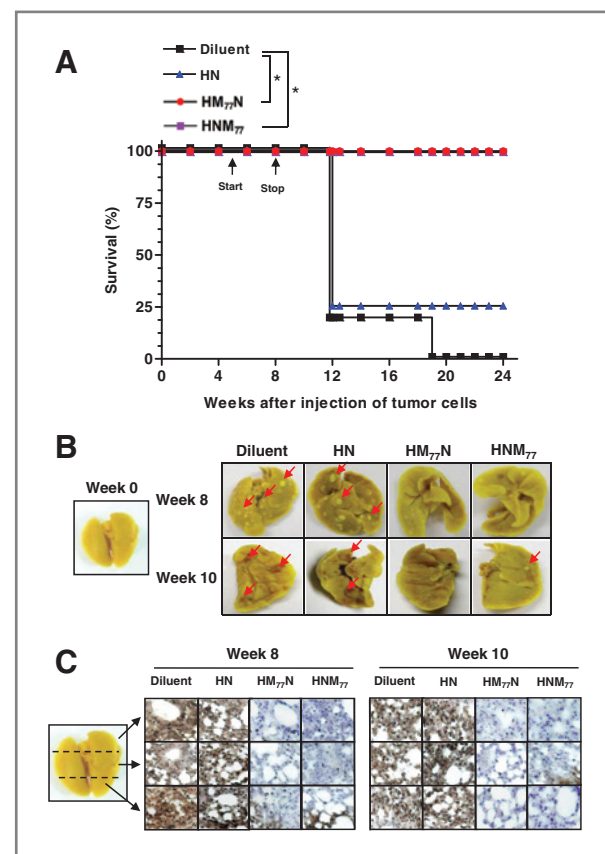

Figure 5. CP-NM23 suppresses established metastases. A, Kaplan–Meier plots comparing MDA-MB-435–injected mice treated with diluent (black square) or 300 μg/mouse/day of recombinant NM23 proteins (HN: blue triangle, $HM_{77}N$: red circle, or HNM_{77}: magenta square). $n = 10$; *, $P < 0.05$, as determined by the Student *t* test. B, lungs from mice were fixed in Bouin`s solution. C, immunohistology of vimentin expression.

cells (Supplementary Fig. S4). To determine the effects of CP-NM23 on p53-dependent apoptosis and angiogenesis, 3 different human cancer cell lines originating from breast (MDA-MB-435), colon (HCT116), and lung (A549) cells were treated with CP-NM23. $HM_{77}N$ positively regulated the phosphorylation of p53 and negatively controlled the expression of metastasis-specific markers, EDG2 and VEGF (Supplementary Fig. S5). Thus, CP-NM23 suppressed multiple aspects of the metastatic phenotype.

Because metastasis also involves processes extrinsic to tumor cells, including tissue remodeling and angiogenesis, $HM_{77}N$ was also tested for antiangiogenic activity (Supplementary Fig. S6). Primary human vascular endothelial cells treated with buffer alone or control NM23 protein (HN) spontaneously organized into tubes when cultured on a Matrigel substrate, whereas $HM_{77}N$ effectively blocked tube formation.

Systemic delivery of CP-NM23

Systemic delivery of CP-NM23 was examined in mice following i.v. injection of FITC-labeled $HM_{77}N$. High levels of FITC-$HM_{77}N$ were observed in peripheral blood leukocytes/lymphocytes, total splenocytes, and liver and spleen cryosections within 1 hour after injection. The protein persisted for several hours as assessed by flow cytometry (Fig. 4A), fluorescence microscopy (Fig. 4B), and immunostaining with antibodies specific for either NM23 (Fig. 4C, left) or the His-peptide tag (Fig. 4C, right). In contrast, the same cells and tissues failed to accumulate FITC alone or FITC-labeled NM23 protein lacking the MTD-77 sequence (FITC-HN). The half-lives of internalized MTD-fused recombinant NM23 proteins in PBMC and spleen cells were 4.5 and 2.8 hours, respectively (D. Jo et al., manuscript in preparation). These results show the ability of MTD-77 to deliver a biologically active NM23 fusion protein to multiple cells and tissues.

CP-NM23 enhances survival of mice with disseminated metastases

We next tested CP-NM23 for antitumor activity in xenograft metastasis models. MDA-MB-435 cells, a metastatic human breast-cancer cell line, were injected (5×10^6) into the lateral tail veins of 5-week-old, MHC-deficient Balb/c nu/nu mice, and after 5 weeks, 10 mice each were treated daily with diluent alone or with 300 μg HN, $HM_{77}N$, or HNM_{77} proteins for 3 weeks (weeks 5–8). Animal survival was monitored for 24 weeks (Fig. 5A). $HM_{77}N$ and HNM_{77} proteins both greatly enhanced survival as compared with that of controls ($P < 0.05$). Consistent with differences in survival, mice treated with CP-NM23 proteins contained far fewer lung metastases at the end of the treatment period at week 8 (Fig. 5B, top) and 2 weeks later (Fig. 5B, bottom) than lungs from mice treated with diluent alone or with NM23 protein without a MTD sequence. These macroscopic differences were confirmed by a histologic examination of lung sections immunostained for vimentin, a marker of tumor invasiveness (Fig. 5C). Similar or greater survival differences between $HM_{77}N$ treatment and controls were obtained when the experiment was extended for 40 weeks (Fig. 6A; $P < 0.001$) and when mice were treated twice weekly instead of daily (Fig. 6B; $P < 0.001$). As before, lungs from control mice contained greater numbers of visible vimentin-expressing metastases at week 8 as compared with $HM_{77}N$-treated mice (Fig. 6C and D). Similar results were obtained following tail vein injection of 5×10^6 MDA-MB-231 cells in fewer animals (5 per treatment group, data not shown).
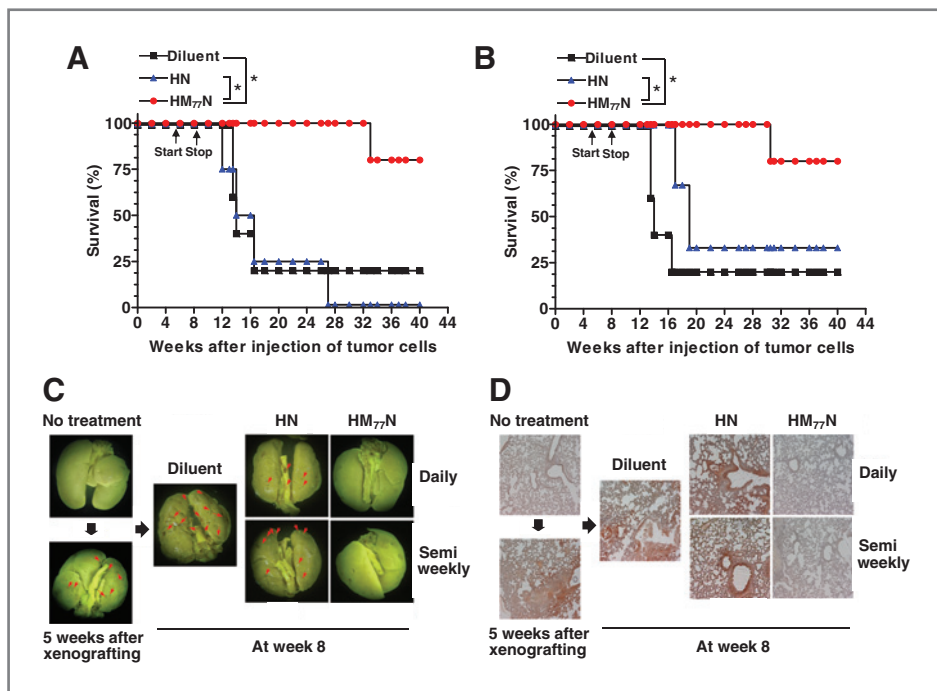

Figure 6. CP-NM23 promotes long-term survival in mice with established pulmonary metastases. A and B, Kaplan–Meier plots comparing MDA-MB-435–injected mice treated daily (A) or semiweekly (B). $n = 10$; *, $P < 0.001$, as determined by the Student t test. Start and Stop arrows indicate the start and stop of protein treatment (from week 5m to 8 after i.v. injection of cancer cells). C, lungs isolated at weeks 0, 5, and 8 were photographed showing metastases (indicated by an arrow). D, immunohistology of vimentin expression.

These results show that protein therapy with CP-NM23 significantly inhibits the growth and persistence of well-established breast cancer metastases *in vivo*, resulting in increased survival. To test whether CP-NM23 can inhibit the seeding of tumor metastases, protein therapy was initiated at the same time mice were injected with MDA-MB-435 tumor cells. Mice injected daily with $HM_{77}N$ exhibited enhanced survival (90%) after 40 weeks as compared with control mice (20%; Fig. 7A), and remained virtually free of metastases at weeks 3, 8, 13, and 20 (Fig. 7B and C). These results suggest that CP-NM23 inhibits the initial seeding of metastatic cancer cells as well as the growth and persistence of established tumors.

Discussion

Metastasis is an important clinical problem responsible for the vast majority of all cancer deaths, including a high percentage of therapeutic failure following curative resection. For example, the 5-year recurrence rate for lymph node–negative colon, lung, and breast/prostate cancers is 30%, 40%, and 10% to 20%, respectively (2). Adjuvant therapies capable of arresting or reversing the metastatic process are therefore expected to have a significant impact on cancer mortality. In the present study, we show the effectiveness of protein-based therapy to deliver CP-NM23 protein as an antimetastatic agent. The CP-NM23 inhibited metastasis associated phenotypes in tumor cell lines and not only suppressed the establishment of lung metastases but also cleared already established metastases, greatly prolonging the survival of animals harboring disseminated tumor cells.

Our approach made use of new MTDs designated MTD-76 and MTD-77, which were selected from a screen of 1,500 hydrophobic signaling peptides and subsequently modified to eliminate charged and polar amino acids, increase predicted α-helical content and limit the number of consecutive hydrophobic residues (D. Jo et al., manuscript in preparation). In the present study, MTD-76 and MTD-77 significantly improved (up to 4-fold) the delivery of recombinant proteins into cultured cells and tissues as compared with the hydrophobic transduction domain based on the FGF-4 signal peptide. These data establish MTD-76 and MTD-77 as potential vectors for protein-based therapeutics.

Our decision to investigate hydrophobic MTDs rather than use basic protein transduction domains (e.g., HIV tat) was based on several considerations. First, previous studies had made only a limited effort to identify hydrophobic sequences with enhanced protein transduction activity (18). Second, despite this limitation, the FGF-4 MTD has been successfully used to deliver biologically active peptides and proteins systemically in animals including dramatic protection to lethal proinflammatory conditions (20, 22–24). Finally, the hydrophobic MTDs are thought to enter cells directly by penetrating the plasma membrane; (18) in contrast, the basic protein transduction domains bind to the cell surface and bulk entry occurs by endocytosis (25). Although these distinctions are not absolute and uptake mechanisms may vary depending on the cargo, we were concerned that endocytosed proteins that fail to reach the cytosol (26) could
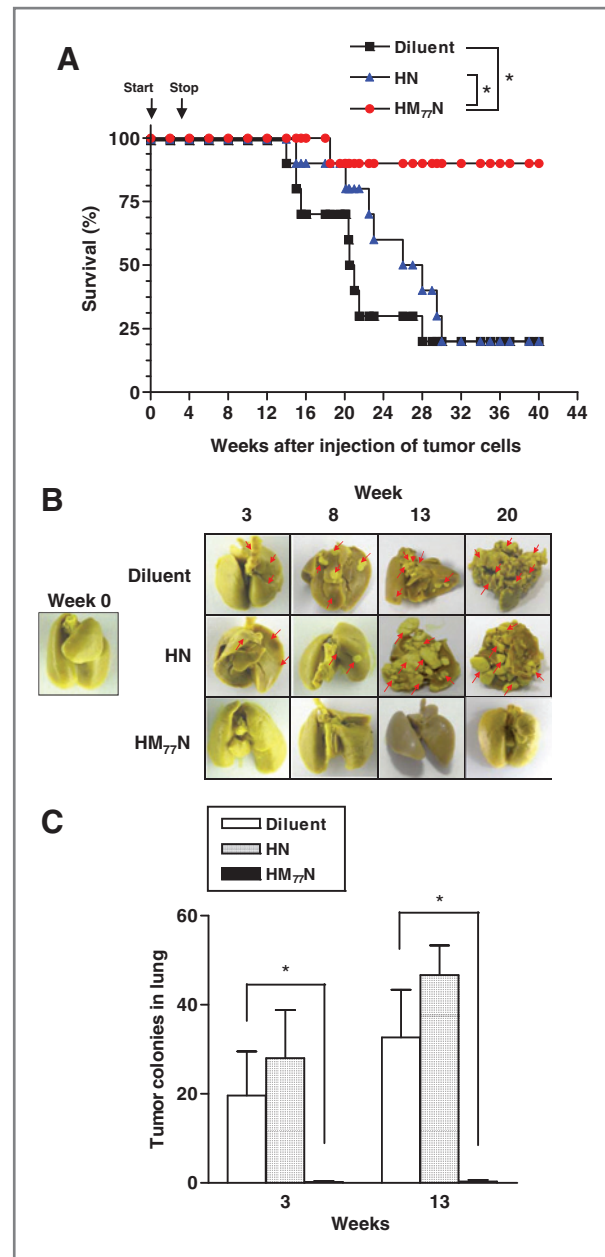

Figure 7. CP-NM23 blocked the establishment of metastases. A, Kaplan–Meier plots of mice treated in a prophylactic protocol. Mice were injected with MDA-MB-435 tumor cells and were immediately treated with recombinant NM23 proteins daily for 3 weeks. $n = 10$; *, $P < 0.05$, as determined by the Student t test. B, lungs fixed in the Bouin solution. C, visible tumor colonies (>1 mm length) were counted at week 3 and 13. $n = 5$; *, $P < 0.01$, as determined by the Student t test.

limit the bioavailability of proteins with basic transduction domains (27).

CP-NM23 protein suppressed multiple metastasis-associated phenotypes in cultured tumor cells including cell migration, adhesion, and Matrigel invasion, and blocked angiogenic tube formation by vascular endothelial cells. These effects were accompanied by reductions in MAPK signaling (notably MEK

and ERK phosphorylation), EDG2 expression, and enhanced apoptosis, consistent with the effects of augmented NM23 gene expression in cultured cells (11, 13–15, 28). In principle, such activities are expected to suppress multiple early events in the metastatic process such as invasion, attachment, colonization, and neovascularization. Indeed, CP-NM23 blocked the seeding of pulmonary metastases when administered at the time tumor cells were introduced into the blood stream. Moreover, CP-NM23 also targeted already established metastases, in some cases clearing the lungs of tumors and greatly increasing survival.

The levels of metastasis suppression achieved by CP-NM23 were comparable with if not greater than those reported after enforced expression of the NM23 gene in tumor cell lines (6–10). This suggests that the activity of systemically delivered MTD-77-NM23 approaches theoretical limits determined by the biology of the NM23 function in tumor cells. MTD-77-NM23 also outperformed gene therapy (29, 30) and hormonal activation of the endogenous NM23 gene (12). The latter study, which provided the basis for human trials of medroxyprogesterone acetate, reported 55% fewer lung metastases in treated mice after 14 weeks, whereas, most mice treated with cell-permeable NM23 remained free of lung metastases even after 20 weeks. Moreover, while medroxyprogestrone-treated mice maintained weight better (by 18% after 14 weeks), we observed far more dramatic survival differences after 40 weeks (80%–100% treated animals survived vs. 0%–25% of mice in the control groups). These results underscore the ability of MTD-77 to systemically deliver biologically active proteins into blood-borne tumor cells and metastases. Moreover, in addition to targeting tumor cells, the efficacy of CP-NM23 as a metastasis suppressor may benefit from targeting other cells and processes required to establish and maintain metastases in ectopic tissue niches.

Although NM23-H1 was initially characterized as a metastasis suppressor, the protein functions in normal hematopoiesis (31, 32) and plays complex roles in the development of different malignancies (33). Moreover, NM23-H1 functions are not always intracellular, judging from activities mediated by extracellular NM23 (34, 35). In particular, the protein is overexpressed in some tumors, including hematologic malignancies, and is present at elevated levels in patient sera, where the protein seems to promote tumor cell growth and survival by autocrine and/or paracrine mechanisms (36–39). In the present study, we show that NM23-H1 lacking an MTD sequence does not efficiently enter cells. This underscores the idea that the biologic effects of externally applied NM23 protein originate from outside the cell and not from internalized protein. Even so, considering the widespread ability of proteins to enter cells (40), studies investigating extracellular HM23 should examine this issue more carefully. Conversely, the antimetastatic function of HM23, which strictly required an MTD sequence, seems to be mediated by intracellular protein. However, although the MTD sequence and protein internalization seem necessary, they may not be sufficient for the full antimetastatic response. Additional experiments will be required to determine if extracellular NM23, for example acting on myeloid cells, contributes to the antimetastatic response.

In summary, despite widespread interest in metastasis as a therapeutic target, most antimetastatic drugs currently in development focus on tumor cell migration and invasion with uncertain utility against disseminated disease (41). Our results describe a potential therapeutic strategy to target occult metastases that are resistant to conventional chemotherapy.

Disclosure of Potential Conflicts of Interest

Acknowledgments

Grant Support

References

1. Nguyen DX, Bos PD, Massague J. Metastasis: from dissemination to organ-specific colonization. Nat Rev Cancer 2009;9:274–84.
2. Riethdorf S, Wikman H, Pantel K. Review: biological relevance of disseminated tumor cells in cancer patients. Int J Cancer 2008;123:1991–2006.
3. Smith SC, Theodorescu D. Learning therapeutic lessons from metastasis suppressor proteins. Nat Rev Cancer 2009;9:253–64.
4. Marshall JC, Collins J, Marino N, Steeg P. The Nm23-H1 metastasis suppressor as a translational target. Eur J Cancer 2010;46:1278–82.
5. Hartsough MT, Steeg PS. Nm23/nucleoside diphosphate kinase in human cancers. J Bioenerg Biomembr 2000;32:301–8.
6. Leone A, Flatow U, King CR, Sandeen MA, Margulies IM, Liotta LA, et al. Reduced tumor incidence, metastatic potential, and cytokine responsiveness of nm23-transfected melanoma cells. Cell 1991;65:25–35.
7. Leone A, Flatow U, VanHoutte K, Steeg PS. Transfection of human nm23-H1 into the human MDA-MB-435 breast carcinoma cell line: effects on tumor metastatic potential, colonization and enzymatic activity. Oncogene 1993;8:2325–33.

8. Parhar RS, Shi Y, Zou M, Farid NR, Ernst P, al-Sedairy ST. Effects of cytokine-mediated modulation of nm23 expression on the invasion and metastatic behavior of B16F10 melanoma cells. Int J Cancer 1995;60:204–10.

9. Baba H, Urano T, Okada K, Furukawa K, Nakayama E, Tanaka H, et al. Two isotypes of murine nm23/nucleoside diphosphate kinase, nm23-M1 and nm23-M2, are involved in metastatic suppression of a murine melanoma line. Cancer Res 1995;55:1977–81.

10. Miyazaki H, Fukuda M, Ishijima Y, Takagi Y, Iimura T, Negishi A, et al. Overexpression of nm23-H2/NDP kinase B in a human oral squamous cell carcinoma cell line results in reduced metastasis, differentiated phenotype in the metastatic site, and growth factor-independent proliferative activity in culture. Clin Cancer Res 1999;5:4301–7.

11. Hartsough MT, Morrison DK, Salerno M, Palmieri D, Ouatas T, Mair M, et al. Nm23-H1 metastasis suppressor phosphorylation of kinase suppressor of Ras via a histidine protein kinase pathway. J Biol Chem 2002;277:32389–99.

12. Palmieri D, Halverson DO, Ouatas T, Horak CE, Salerno M, Johnson J, et al. Medroxyprogesterone acetate elevation of Nm23-H1 metastasis suppressor expression in hormone receptor-negative breast cancer. J Natl Cancer Inst 2005;97:632–42.

13. Otsuki Y, Tanaka M, Yoshii S, Kawazoe N, Nakaya K, Sugimura H. Tumor metastasis suppressor nm23H1 regulates Rac1 GTPase by interaction with Tiam1. Proc Natl Acad Sci U S A 2001;98:4385–90.

14. Palacios F, Schweitzer JK, Boshans RL, D'Souza-Schorey C. ARF6-GTP recruits Nm23-H1 to facilitate dynamin-mediated endocytosis during adherens junctions disassembly. Nat Cell Biol 2002;4:929–36.

15. Murakami M, Meneses PI, Knight JS, Lan K, Kaul R, Verma SC, et al. Nm23-H1 modulates the activity of the guanine exchange factor Dbl-1. Int J Cancer 2008;123:500–10.

16. Jung H, Seong HA, Ha H. Direct interaction between NM23-H1 and macrophage migration inhibitory factor (MIF) is critical for alleviation of MIF-mediated suppression of p53 activity. J Biol Chem 2008;283:32669–79.

17. Kaetzel DM, McCorkle JR, Novak M, Yang M, Jarrett SG. Potential contributions of antimutator activity to the metastasis suppressor function of NM23-H1. Mol Cell Biochem 2009;329:161–5.

18. Hawiger J. Noninvasive intracellular delivery of functional peptides and proteins. Curr Opin Chem Biol 1999;3:89–94.

19. Jo D, Lin Q, Nashabi A, Mays DJ, Unutmaz D, Pietenpol JA, et al. Cell cycle-dependent transduction of cell-permeant Cre recombinase proteins. J Cell Biochem 2003;89:674–87.

20. Jo D, Liu D, Yao S, Collins RD, Hawiger J. Intracellular protein therapy with SOCS3 inhibits inflammation and apoptosis. Nat Med 2005;11:892–8.

21. Jo D, Nashabi A, Doxsee C, Lin Q, Unutmaz D, Chen J, et al. Epigenetic regulation of gene structure and function with a cell-permeable Cre recombinase. Nat Biotechnol 2001;19:929–33.

22. Moore DJ, Zienkiewicz J, Kendall PL, Liu D, Liu X, Veach RA, et al. In vivo islet protection by a nuclear import inhibitor in a mouse model of type 1 diabetes. PLoS One 2010;5:e13235.

23. Liu D, Liu XY, Robinson D, Burnett C, Jackson C, Seele L, et al. Suppression of staphylococcal enterotoxin B-induced toxicity by a nuclear import inhibitor. J Biol Chem 2004;279:19239–46.

24. Chow NH, Liu HS, Chan SH. The role of nm23-H1 in the progression of transitional cell bladder cancer. Clin Cancer Res 2000;6:3595–9.

25. Gump JM, Dowdy SF. TAT transduction: the molecular mechanism and therapeutic prospects. Trends Mol Med 2007;13:443–8.

26. Raagel H, Saalik P, Pooga M. Peptide-mediated protein delivery-Which pathways are penetrable? Biochim Biophys Acta 2010;1798:2240–8.

27. Sarko D, Beijer B, Boy RG, Nothelfer EM, Leotta K, Eisenhut M, et al. The pharmacokinetics of cell-penetrating peptides. Mol Pharm 2010;7:2224–31.

28. Murakami M, Meneses PI, Lan K, Robertson ES. The suppressor of metastasis Nm23-H1 interacts with the Cdc42 Rho family member and the pleckstrin homology domain of oncoprotein Dbl-1 to suppress cell migration. Cancer Biol Ther 2008;7:677–88.

29. Damo LA, Snyder PW, Franklin DS. Tumorigenesis in p27/p53- and p18/p53-double null mice: functional collaboration between the pRb and p53 pathways. Mol Carcinog 2005;42:109–20.

30. Bitler BG, Schroeder JA. Anti-cancer therapies that utilize cell penetrating peptides. Recent Pat Anticancer Drug Discov 2010;5:99–108.

31. Arnaud-Dabernat S, Bourbon PM, Dierich A, Le Meur M, Daniel JY. Knockout mice as model systems for studying nm23/NDP kinase gene functions. Application to the nm23-M1 gene. J Bioenerg Biomembr 2003;35:19–30.

32. Postel EH, Zou X, Notterman DA, La Perle KM. Double knockout Nme1/Nme2 mouse model suggests a critical role for NDP kinases in erythroid development. Mol Cell Biochem 2009;329:45–50.

33. Kaul R, Murakami M, Kumar P, Robertson ES. Nm23 as a metastasis inhibitor. In: Thomas-Tikhonenko A, editor. Cancer genome and tumor microenvironment. New York: Springer Science + Business Media, LLC; 2010. p. 233–71.

34. Okabe-Kado J, Kasukabe T, Hozumi M, Honma Y, Kimura N, Baba H, et al. A new function of Nm23/NDP kinase as a differentiation inhibitory factor, which does not require it's kinase activity. FEBS Lett 1995;363:311–5.

35. Willems R, Slegers H, Rodrigus I, Moulijn AC, Lenjou M, Nijs G, et al. Extracellular nucleoside diphosphate kinase NM23/NDPK modulates normal hematopoietic differentiation. Exp Hematol 2002;30:640–8.

36. Niitsu N, Okabe-Kado J, Nakayama M, Wakimoto N, Sakashita A, Maseki N, et al. Plasma levels of the differentiation inhibitory factor nm23-H1 protein and their clinical implications in acute myelogenous leukemia. Blood 2000;96:1080–6.

37. Mahanta S, Fessler SP, Park J, Bamdad C. A minimal fragment of MUC1 mediates growth of cancer cells. PLoS One 2008;3:e2054.

38. Okabe-Kado J, Kasukabe T, Honma Y, Kobayashi H, Maseki N, Kaneko Y. Extracellular NM23 protein promotes the growth and survival of primary cultured human acute myelogenous leukemia cells. Cancer Sci 2009;100:1885–94.

39. Lilly AJ, Khanim FL, Hayden RE, Luong QT, Drayson MT, Bunce CM. Nm23-h1 indirectly promotes the survival of acute myeloid leukemia blast cells by binding to more mature components of the leukemic clone. Cancer Res 2011;71:1177–86.

40. Heitz F, Morris MC, Divita G. Twenty years of cell-penetrating peptides: from molecular mechanisms to therapeutics. Br J Pharmacol 2009;157:195–206.

41. Mack GS, Marshall A. Lost in migration. Nat Biotechnol 2010;28:214–29.